JOC The Journal of Organic Chemistry

Article

pubs.acs.org/joc

Regioselective Acetylation of Diols and Polyols by Acetate Catalysis: Mechanism and Application

Bo Ren,[†] Martin Rahm,*[,‡,§] Xiaoling Zhang,[†] Yixuan Zhou,[†] and Hai Dong*[,†]

[†]Key Laboratory for Large-Format Battery Materials and System, Ministry of Education, School of Chemistry & Chemical Engineering, Huazhong University of Science & Technology, Luoyu Road 1037, Wuhan 430074, People's Republic of China

[‡]Department of Chemistry and Chemical Biology, Cornell University, Baker Laboratory, Ithaca 14853, New York, United States

[§]Department of Applied Physical Chemistry, KTH-Royal Institute of Technology, Teknikringen 30, 10044 Stockholm, Sweden

Supporting Information

ABSTRACT: We propose a principle for H-bonding activation in acylation of hydroxyl groups, where the acylation is activated by the formation of hydrogen bonds between hydroxyl groups and anions. With the guidance of this principle, we demonstrate a method for the selective acylation of carbohydrates. By this method, diols and polyols are regioselectively acetylated in high yields under mild conditions using catalytic amounts of acetate. In comparison to other methods involving reagents such as organotin, organoboron, organosilicon, organobase, and metal salts, this method is more environmentally friendly, convenient, and efficient and is also associated with higher regioselectivity. We have performed a thorough quantum chemical study to decipher the mechanism, which suggests that acetate first forms a dual H-bond complex with a diol, which enables subsequent monoacylation by acetic anhydride under mild conditions. The regioselectivity appears to originate from the inherent structure of the diols and polyols and their specific interactions with the coordinating acetate catalyst.

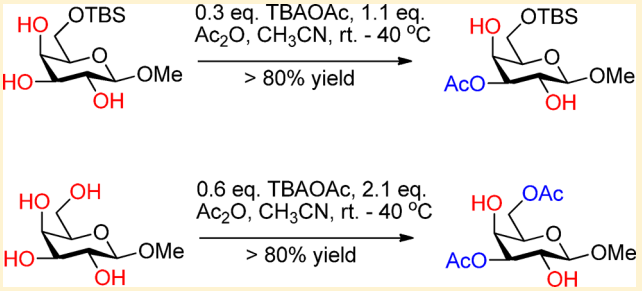

INTRODUCTION

It is a prominent challenge to develop a green, convenient, and highly efficient regioselective carbohydrate protection method in synthetic carbohydrate chemistry.[1−3] Selectively protected monosaccharides can act as both value-added intermediates and building blocks for further use in glycosylation reactions.[4,5] Efficient methods using organotin reagents have been widely employed in the past few decades.[6−12] However, the employment of organotin reagents has recently been limited due to their potential inherent toxicity.[13−15] For this reason, some methods were developed in which only catalytic amounts of organotin reagents were used[9−12] or in which nontoxic alternatives to common organotin reagents can be employed.[16−19] One important breakthrough was the discovery of organoboron reagents, which exhibit low toxicity and can be used in catalytic amounts.[16−18] However, large amounts of organobase are necessary in this method for neutralization. In addition, only carbohydrate derivatives containing a *cis*-vicinal diol motif can be selectively protected by this method. We recently proposed a principle for organotin-mediated regioselective carbohydrate protection in which the regioselectivity is likely to be controlled by steric and stereoelectronic effects of the parent substrate structure.[7,20] Under the guidance of this principle, an organosilicon-mediated regioselctive acetylation of carbohydrates was developed.[19] The regioselective protection patterns are the same as those of organotin-mediated acylation methods, while enabling similar yields. Although organosilicon reagents are associated with lower cost and lower toxicity and are more easily acquired, this method is not very convenient, due to the formation of cyclic dioxasilolane- or dioxasilinane-type intermediates prior to the acetylation. Some other methods involving heavy-metal salts,[21−24] organocatalysis,[25−27] and enzymes[28−31] also have their respective shortcomings, with respect to convenience, efficiency, and environmentally sustainable conditions.

Yoshida et al. may have been the first to rationalize the regioselectivity observed in base-catalyzed acylation reactions of polyols to the interplay of hydrogen-bonding interactions within polyol substrates and carboxylate counterions.[32,33] Albert et al. further rationalized the acetylation regioselectivity by dual H-bonding complexes formed between polyol substrates and carboxylate counterions.[34] Spivey et al.[35] and Kawabata et al.[36] have discussed the role of carboxylate ions as the only relevant base for deprotonating the reacting hydroxy groups. These studies utilized a highly electrophilic N-acylpyridinium counterion intermediate as the acyl donor. We recently reported on the application of H-bonding activation in a highly regioselective acetylation of diols (Scheme 1).[37] On the basis of our results, it appears that H bonding between hydroxyl groups and anions can activate acetylation in the absence of a pyridine catalyst and lead to higher regioselectivities. In our

Received: June 16, 2014
Published: August 7, 2014

   dx.doi.org/10.1021/jo501343x | J. Org. Chem. 2014, 79, 8134−8142

Scheme 1. Regioselective Acetylation of Diols Catalyzed by Acetate Anion

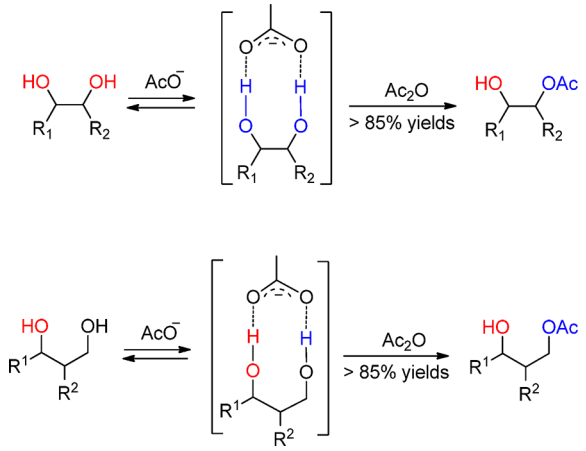

study, catalytic amounts of tetrabutylammonium acetate (0.3 equiv) were employed to form H-bonding complexes with diols, leading to regioselective acetylation of the diols by acetic anhydride. These reactions were performed under mild conditions without the assistance of any other reagents. Following an ^{1}H NMR study and a tentative quantum chemical investigation, we proposed a mechanism which involves an initial formation of a dual H-bonded complex between the acetate anion and the diol.[37] On this basis, we speculated that the resulting regioselectivities might also be controlled by steric and stereoelectronic effects of the parent substrate structure, similar to the organotin cases. Especially, the regioselectivity might originate from the inherent structure of the diol−acetate H-bonded complex. To the best of our knowledge, this method is the most convenient, green, efficient, economical, and regioselective high-yield acetylation method to date. Therefore, the origin of the regioselectivity needs to be further elucidated.

In addition, of particular importance is the possibility of acquiring single or multiple protections for polyols in single-step processes. The disbutylstannylene-mediated multiple carbohydrate esterification requires an excess (2−3 equiv) of organotin reagent.[38] We wondered if the acetylation activation method, which supposedly proceeds via dual H bonding, could be applied in single or multiple esterification for polyols, where a catalytic amount of TBAOAc (0.3−0.6 equiv) would be used instead of organotin. We here present the results of an extensive quantum chemical study of the catalytic system alongside further application of the methodology.

RESULTS AND DISCUSSION

One classic method for the acetylation of a free glycoside involves pyridine together with an acetylation reagent, such as acetyl chloride (AcCl) or acetic anhydride (Ac_2O). The high rate of this reaction prohibits adequate regioselectivity, unless very low reaction temperatures (<−40 °C) are used.[39] In light of a consensus mechanism (Figure 1a), pyridine initially forms a highly electrophilic *N*-acylpyridinium counterion with the acetylation reagent.[40−42] The acylpyridinium ion then reacts with the hydroxyl groups. It has been found that the counterion has a strong effect on the reaction rate and that more basic counterions lead to faster reaction rates (CN > OAc > Cl) for DMAP-catalyzed acetylation.[34,43]

We have also found that the acetylation of hydroxyl groups by Ac_2O is much faster than when AcCl is used in a pyridine-catalyzed acetylation (Table 1). However, the reason for this is still not very clear. In an earlier study, we found that intramolecular acetyl group migration can be activated by anions in nonpolar solvents under mild conditions.[45] The leading cause for this process has been attributed to the formation of hydrogen bonds between neighboring hydroxyl groups and anions. The catalytic effect of anions follows the corresponding H-bond formation tendencies, where more basic

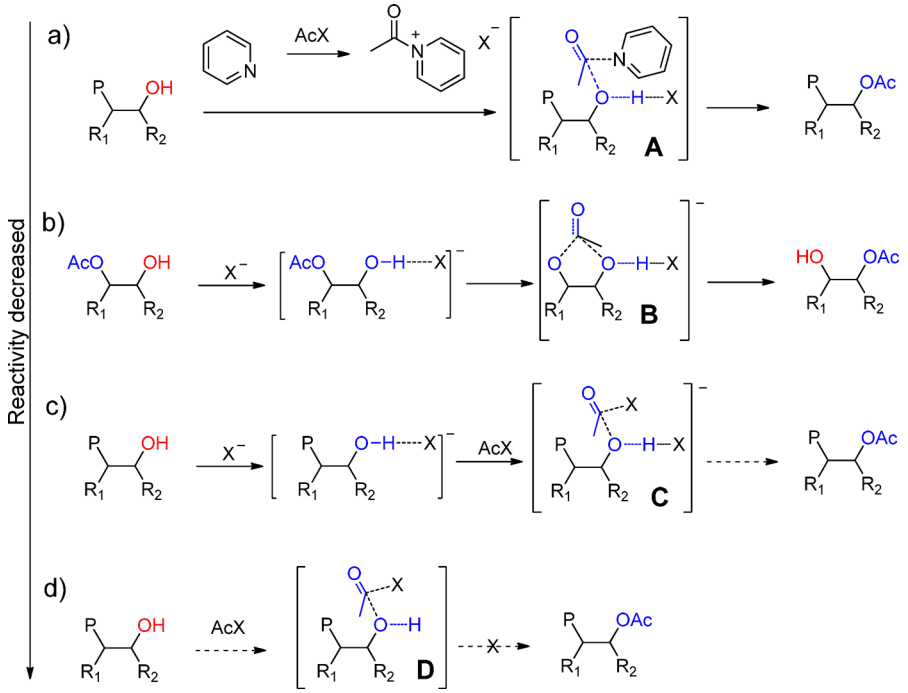

Figure 1. Anion-promoted acetylations by the formation of hydrogen bonding.

dx.doi.org/10.1021/jo501343x | J. Org. Chem. 2014, 79, 8134−8142

Table 1. Comparison of the Acetylation Rates in Pyridine-Catalyzed Acetylations[a]

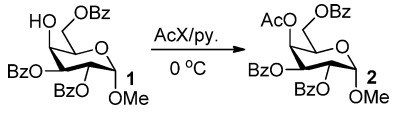

entry	reagent (2.0 equiv)	solvent	base (2.0 equiv)	time/h	conversion/%
1	AcCl	Py		1	17
2	Ac_2O	Py		1	50
3	AcCl	DCM	Py	1	24
4	Ac_2O	DCM	Py	1	31

[a]Reaction conditions: 50 mg of reactant in 1 mL of solvent, 0 °C, 1 h.

anions lead to faster migration. A proposed mechanism is shown in Figure 1b.

Calculations at the B3LYP/6-311+G(d,p)//6-31G(d) level suggest that **A** in Figure 1a corresponds to the rate-determining transition state structure.[41] Similarly, **B** in Figure 1b is believed to be the rate-determining transition state structure in acetyl group migration. Due to the stabilizing electrophilic *N*-acylpyridinium in structure **A**, the energy of **A** is lower than that of **B**. This explains why the rate of pyridine-catalyzed acetylation is higher than that of anion-activated acetyl group migration. As for the acetylation without the catalysis of pyridine (Figure 1d), a destabilized transition state structure **D** will not allow for acetylation. In the transition structure types **A** and **B**, stronger H bonding makes the oxygen atom of the hydroxyl group more negatively charged, leading to further stabilization of the transition state. Consequently, with fluoride, acetate, chloride, and bromide anions, the energies of **A** and **B** should follow the order $\mathbf{A}_1 < \mathbf{A}_2 < \mathbf{A}_3 < \mathbf{A}_4$ and $\mathbf{B}_1 < \mathbf{B}_2 < \mathbf{B}_3 < \mathbf{B}_4$ (Figure 2). Arguably, this could explain the results in Table 1, in DMAP-catalyzed acetylation[34,43,44] and in H-bond-activated intramolecular acetyl group migration.[45]

On the basis of this analysis, an interesting question emerges: what will happen if the *N*-acylpyridinium ion in the transition state of type **A** is replaced by an acetylation reagent? In this case, the reaction will go through the transition state **C** (Figure 1c). The barrier height corresponding to structure **C** should be similar to that of structure **B**, since their structures are very similar (Figure 2). Thus, acetylation reactions may proceed with the addition of anions under the same conditions as anion-activated acetyl group migration, and furthermore, the acetylation may show regioselectivity, since its reactivity is much lower than that of pyridine-catalyzed acetylation. To investigate this hypothesis, a diol model was tested in acetylation with the addition of Ac_2O and various anions.[37] Our studies indeed indicated that the acetylation could be activated by the formation of H bonds between hydroxyl group and anions and that more basic anions lead to faster acetylation. A range of diols were allowed to react with 1.1 equiv of Ac_2O in the presence of 0.3 equiv of TBAOAc in acetonitrile at 40 °C for 8−24 h.[37] This resulted in high regioselectivities in most cases and excellent isolated yields, indicating that the diols can be regioselectively acetylated when acetate is employed as a catalyst. Though our initial mechanistic studies included a preliminary quantum chemical study, which supported a dual H-bond model as a viable explanation for the catalytic activity of acetate and the origin of the regioselectivity, a more extensive quantum chemical study was still deemed necessary.

Mechanistic Study. We chose 1,2-propanediol (**3**) as an initial model system (Figure 3). To investigate possible additional influences by sterics and dispersion forces, the model was later expanded to a carbohydrate structure with the identical diol structural motif (Figure 4). In order to reduce the size of the calculation, the benzyl groups in 2- and 6-positions in compound **6** were substituted with methyl groups, giving the model carbohydrate (**M**). Geometry optimization and frequency analysis were performed using Gaussian 09[46] at the M06-2X[47]/6-31+G(d,p) level of theory. Acetonitrile solvent was treated implicitly by the SMD-PCM[48] method. This was followed by single-point energy calculations at several levels of theory. The B2PLYP double hybrid and the M06-2X hybrid meta exchange DFT functionals have been extensively tested in large test sets and have reported mean absolute energy deviations of 2.5[49] and 2.2 kcal/mol,[50] respectively.

We found no meaningful differences (<0.4 kcal/mol) when comparing the TZVP with the Def2-TZVPP basis sets in the small 1,2-propanediol model (Table S1, Supporting Informa-

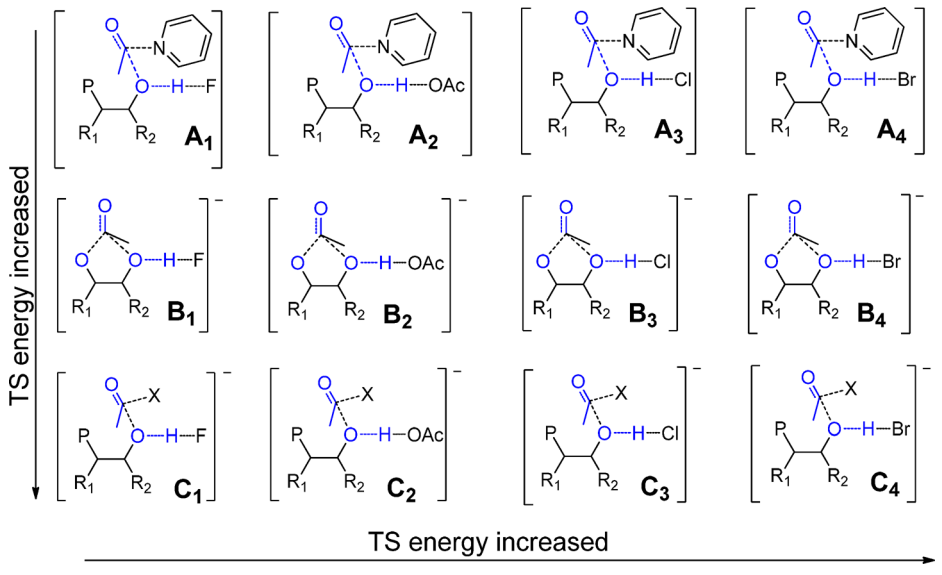

Figure 2. Proposed energy order of the rate-determining transition structures.

dx.doi.org/10.1021/jo501343x | J. Org. Chem. 2014, 79, 8134−8142

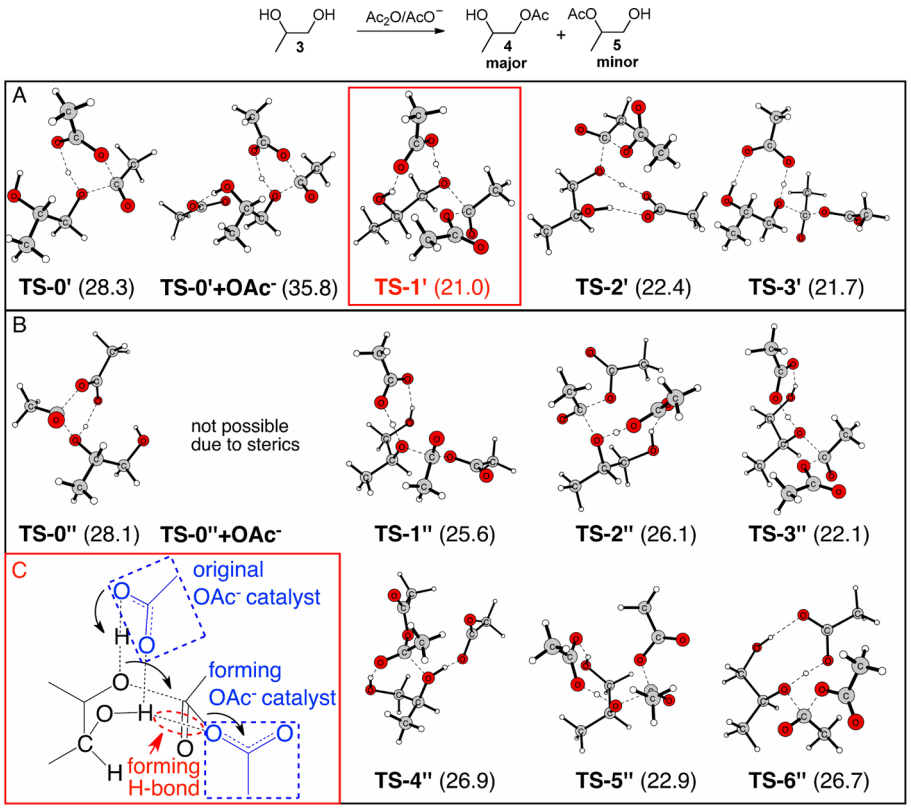

Figure 3. The model reaction of 1,2-propanediol is given at the top. (A, B) Considered transition state geometries for the reaction of 1,2-propanediol with acetic anhydride at (A) the primary position and (B) the secondary position. Reactions at the primary and secondary positions are denoted with ′ and ″, respectively. The uncatalyzed reaction is shown as 0 (zero). The lowest transition state **TS-1′** is highlighted in red. Free energies of activation ($\Delta G^{\ddagger}$, 298 K, 1 M) are given in parentheses. All energies can be found in Table S1 (Supporting Information). (C) Schematic depiction of the lowest transition state, where formation of a key stabilizing hydrogen bond is shown in red.

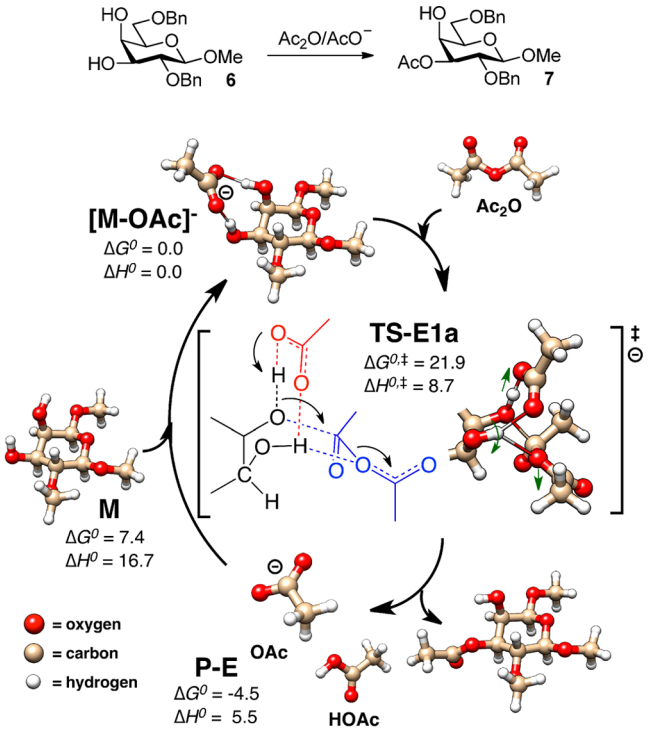

Figure 4. Catalytic cycle for acetylation of the model carbohydrate **M**. Green arrows show nuclear displacements in the transition state. Relative energies (1 M, 298 K) are given in kcal/mol.

tion). However, we were surprised to obtain large (2−4 kcal/mol) differences in transition state energies when comparing SMD-M06-2X with COSMO-B2PLYP-D3 calculations. Therefore, we complemented our study with the range-separated ωB97X-D hybrid functional,[51] which has demonstrated excellent performance for proton transfer kinetics,[52] as well as for general-purpose use.[53] The ωB97X-D functional was found to consistently provide transition state energies between those obtained with M06-2X and B2PLYP-D3. The slightly higher barriers obtained with B2PLYP-D3 and ωB97X-D are in better accord with our experimentally observed rates, and we are inclined to trust these methods more in this case. The differences in the implicit solvation models SMD and COSMO are likely to affect values somewhat, yet large differences were only observed when free (noncomplexed) acetate was considered. It is important to note that the main trends between transition state energies are preserved with all methods, and our conclusion regarding the selectivity of acetylation is unaffected by the choice of method or basis set. For clarity only SMD-ωB97X-D energies are shown in the figures (all results are provided in Table S1, Supporting Information).

To estimate the acidity difference between the competing OH groups, we have calculated the proton affinity of the corresponding alkoxides in acetonitrile solution. The proton affinity of the 2° alkoxide of 1,2-propanediol **3** is found to be 0.3 kcal/mol *higher* using B2PLYP-D3/Def2-TZVPP energies and 0.1 kcal/mol *lower* at the M06-2X/cc-pVTZ level. At the ωB97X-D/cc-pVTZ level the difference in energy is only 0.01

dx.doi.org/10.1021/jo501343x | J. Org. Chem. 2014, 79, 8134−8142

kcal/mol. These results suggest that the acidity difference is minute and is unlikely to affect the acetylation of 1,2-propanediol. For the carbohydrate model all three methods agree that the axial alkoxide has a slightly lower proton affinity (i.e., that the axial OH group is more acidic). The proton affinity differences are 0.37, 0.22, and 0.16 kcal/mol when calculated using B2PLYP-D3, ωB97X-D, and M06-2X, respectively. Thus, our results indicate a slight acidity difference, which is acting *against* the observed selectivity.

Figure 3 illustrates the considered transition state geometries in the 1,2-propanediol system. The lowest transition state, and hence the most likely rate-determining step, for reaction at the primary alcohol group was found to be **TS-1′**, which corresponds to a free energy of activation of 21.0 kcal/mol. The lowest competing pathway, i.e. for reaction at the secondary alcohol, was found to be **TS-3″**, which corresponds to a free energy of activation of 22.1 kcal/mol. These values are both reasonable and are in good agreement with observed rates.

The majority of all identified transition states exhibit dual hydrogen bonding between the diol and the acetate anion. The key difference inherent in **TS-1′** lies with the specific arrangement of the acetic anhydride in relation to the two hydrogen bonds. This arrangement permits for motion over the barrier while simultaneously allowing the formation of a hydrogen bond with the newly forming acetate anion, which is being cleaved off the reacting acetic anhydride (Figure 3C). This hydrogen bond forms in a concerted fashion with the progression over the barrier and acts to slightly stabilize the system. The electronics and geometry are so that the corresponding arrangement for reaction at the secondary position (**TS-1″**, Figure 3) is higher in energy, instead causing **TS-3″** to be the lowest barrier for this competing reaction outcome.

Figure 4 depicts the full catalytic cycle when calculated for the model carbohydrate **M**. The thermodynamics and kinetics of this cycle are very similar to those of the 1,2-propanediol case, with near-identical barrier heights. The more stringent steric constraints enforced by the carbohydrate backbone prohibits several transition state geometries identified at higher relative energies in the smaller model. For this reason, and due to its size, a more limited number of transition state structures were evaluated for the larger model (Figure S4, Supporting Information).

The very slight calculated difference in energy between competing pathways of 1.1−1.8 kcal/mol suggests a selectivity of ∼85−95% at 40 °C in favor of acetylation at the primary/axial position. However, as it is difficult to discern the minor product **5** following acetylation of 1,2-propanediol, from the ^{1}H NMR spectra (Figure S1, Supporting Information), we cannot provide an accurate estimate of the exact selectivity. Our experiments with a range of substrates mostly attain an overall yield exceeding 80% (vide infra). We can conclude that out calculations predict a small but distinct difference in reaction rates between competing pathways and appear to predict a general preference for equatorial and primary hydroxyl sites. This preference can in part be explained by the specific structure of the diol−acetate complex, which guides the geometry into that of a highly concerted transition state. In this transition state one carbon−oxygen bond is broken, another is formed, one proton is transferred from the diol to the acetate catalyst, forming HOAc, and a stabilizing hydrogen bond is formed that facilitates the regeneration of the acetate−catalyst from acetic anhydride. (Figure 3C).

The lowest identified transition state with 1,2-propanediol, **TS-1′**, was chosen as a model for kinetic isotope effect (KIE = k_H/k_D) estimation. For our calculations both hydroxyl hydrogens were substituted for deuterium, while all other hydrogens were left the same. SMD-ωB97X-D/cc-pVTZ//SMD-M06-2X/6-31+G(d,p) calculations within the framework of transition-state theory (TST) at 25 °C provided a KIE of 3.10. Due to the dual hydrogen bond and proton-transfer nature of the reaction such a large primary KIE is reasonable. Due to the quite involved nature of the transition state, we have corrected our TST rate estimates for quantum mechanical tunneling effects using the approximation of Skodje and Truhlar.[54] Whereas our TST rates (@1 M and 25 °C) for the two reactions are k_H = 10^{-3} and k_D= 10^{-4} s^{-1}, accounting for tunneling over the **TS-1′** barrier provides corresponding rates of 3.1 e^{-3} and 9.8 e^{-4} s^{-1}, respectively. This translates into transmission coefficients for the nondeuterated and deuterated cases of 1.18 and 1.15, respectively. Our final estimate for the KIE in the acetylation of 1,2-propanediol, including tunneling, is 3.18. It should be noted that the proper inclusion of variational effects, and the consideration of multiple competing transition states, would likely decrease this value somewhat. By substituting only one of the two hydroxyl hydrogens, we can deduce that the KIE should originate nearly completely from the atom being transferred. Changing the isotope of the second hydroxyl group, which in **TS-1′** is rotating to form a hydrogen bond, does not affect the value noticeably. Due to this, and the fact that rapid exchange would render single-H/D substitution on two bordering hydroxyl groups borderline impossible, experimental KIE measurements will not be able to conclusively prove the exact proposed nature of the transition state: i.e., the presence of dual hydrogen bonding.

In an effort to support our computational predictions, we have attempted to measure the KIE by ^{1}H NMR experiments. Our measured KIE value for 1,2-propanediol is around 2.0 under our most rigorous experimental conditions (Figures S2 and S3, Supporting Information). However, despite our best efforts, we cannot properly evaluate the accuracy of this value because trace amounts of water in the reaction mixture are very hard to remove completely. Even very small amounts of water effectively exchange its protons with the deuterons of the sample, which has the effect of reducing the observed KIE. It is furthermore possible that trace amounts of water can interact with the OH/OD groups and affect the reaction mechanism in a manner we have not considered in our theoretical models. Nevertheless, the KIE observed for 1,2-propanediol implies that proton transfer is occurring in the rate-determining step, in agreement with our computational predictions.

Regioselective Acetylation of Polyols. In light of the studies for regioselective acetylation of diols[37] and the above studies of the reaction mechanism, we propose that dual H-bond complexes also can play key roles in the regioselective acetylation of polyols. To investigate this, TBAOAc was tested together with a range of free glycosides and glycerol (cf. Table 2): methyl β-D-glucoside **8**, methyl α-D-glucoside **9**, methyl β-D-galactoside **10**, methyl α-D-galactoside **11**, methyl α-D-mannoside **12**, and methyl β-D-xyloside **13**, six unprotected pyranosides, and glycerol **14**.

When these compounds were allowed to react with 1.1 equiv of acetic anhydride in the presence of 0.3 equiv of TBAOAc in acetonitrile, mixtures of 3-OAc, 6-OAc, and 3,6-di-OAc products were obtained for the acetylation of compounds **8**−**12**, and good selectivities of monoacetylated products were

dx.doi.org/10.1021/jo501343x | J. Org. Chem. 2014, 79, 8134−8142

Table 2. Acetate-Catalyzed Regioselective Acetylation of Unprotected Carbohydrates[a]

Entry	Reactant	Product	Condition	Yield(%)[b]
1	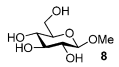	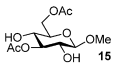	A	83
			B	90
			C	86
2	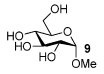	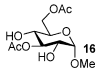	A	78
			B	86
			C	84
3	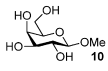	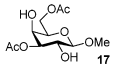	A	84
			B	-[c]
			C	86
4	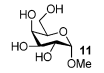	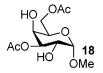	A	85
			B	83
			C	86
5	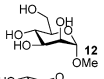	-	A	-[d]
			B	-[c]
			C	-[c]
6	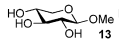	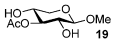	D	93
7	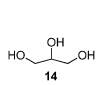	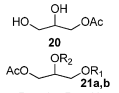	D	71
		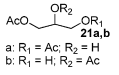 a: R_1 = Ac; R_2 = H b: R_1 = H; R_2 = Ac	A	a/b (70/30)[e]

[a]Reaction conditions: reactant (100 mg), Ac_2O (2.1 equiv), TBAOAc (0.6 equiv); (A) CH_3CN, 40 °C, 8−12 h; (B) CH_3CN, room temperature, 24 h; (C) CH_3CN/DMF (5/1), room temperature, 12−18 h; (D) Ac_2O (1.1 equiv), TBAOAc (0.3 equiv), CH_3CN, 40 °C, 8−12 h. [b]Isolated yield. [c]No reaction. [d]Complex mixture. [e]NMR ratio.

Table 3. Acetate Anion Promoted Monoacetylation of Carbohydrate Derivatives[a]

Entry	Reactant	Product	Condition	Yield(%)[b]
1	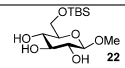	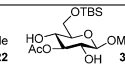	A	80
			B	81
2	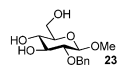	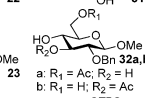 a: R_1 = Ac; R_2 = H b: R_1 = H; R_2 = Ac	A	a/b (75/25)[c]
			C	-[d]
3	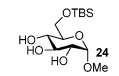	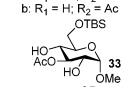	A	82
			B	76
4	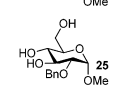	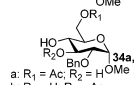 a: R_1 = Ac; R_2 = H b: R_1 = H; R_2 = Ac	A	a/b (29/71)[c]
			C	-[d]
5	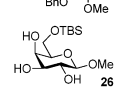	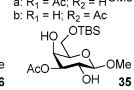	A	79
			B	80
6	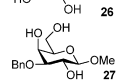	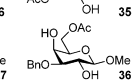	A	85
			B	91
7	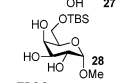	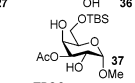	A	80
			B	78
8	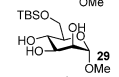	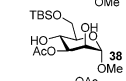	A	83
			B	82
9	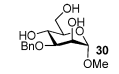	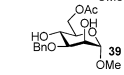	A	83
			B	87

[a]Reaction conditions: reactant (100 mg); (A) Ac_2O (1.1 equiv), TBAOAc (0.6 equiv), CH_3CN, 40 °C, 8−12 h; (B) Ac_2O (1.1 equiv), TBAOAc (0.3 equiv), CH_3CN, 40 °C, 8−12 h; (C) Ac_2O (2.1 equiv), TBAOAc (0.6 equiv), CH_3CN, 40 °C, 8−12 h. [b]Isolated yield. [c]NMR ratio. [d]Complex mixture.

obtained for the acetylation of compounds **13** and **14**. When 2.1 equiv of acetic anhydride and 0.6 equiv of TBAOAc were employed under the same conditions, 3,6-di-OAc products (compounds **15**−**18**) were obtained in high isolated yields. The exception was **12**, where the reaction led to complex mixtures. Acetylation of glycerol **14** led to selective acetylation of two primary hydroxyl groups. An important result is the acetylation of methyl β-D-xyloside **13**, in which the monoacetylation product **19** is obtained in 93% yield. This is, to the best of our knowledge, not possible with any other currently known method.

The unprotected glycosides are poorly soluble in acetonitrile, and a small amount of DMF mixed in acetonitrile can improve the solubility and accelerate reaction rates. Reaction at room temperature can improve regioselectivities and improve the isolated yields.

As selectivity toward 3- and 6-positions of unprotected glycosides was observed, we expected glycosides with either of the 3- and 6-positions protected to show good selectivity for the other respective position. We therefore synthesized and further tested the following substrates (Table 3): compounds **22**, **24**, **26**, **28**, and **29**, in which the 6-OH groups of compounds **8**−**12** were silylated, compounds **23** and **25**, in which the 2-OH groups of compounds **8** and **9** were benzylated, and compounds **27** and **30**, in which the 3-OH groups of compounds **10** and **12** were benzylated. As expected, when compounds **22**, **24**, and **26**−**30** were allowed to react with 1.1 equiv of acetic anhydride in the presence of 0.3−0.6 equiv of TBAOAc in acetonitrile, the monoacetylation 3- and 6-OAc products **31**, **33**, and **35**−**39** were obtained in high isolated yields (78−92%). Mixtures of the major 3-OAc and 6-OAc products were also obtained for the monoacetylation of compounds **23** and **25**. However, it is hard to explain why the NMR ratio 6-OAc/3-OAc was 75/25 for β-D-glucoside **23** whereas it was 29/71 for α-D-glucoside **25**. When compounds **23** and **25** were reacted with 2.1 equiv of acetic anhydride in the presence of 0.6 equiv of TBAOAc in acetonitrile, complex mixtures were obtained instead of the expected 3,6-di-OAc products.

In most examples shown in Tables 2 and 3, the isolated yields of the major product are quite good (>80% yield). This directly translates into high regioselectivities (>80%). However, because only very small amounts of side products are formed, and due to the difficulty in isolation of these minor side products, it is difficult to estimate the overall products distribution exactly. For some examples with yields lower than 80%, the product distribution, or regioselectivity, is given as ^1H NMR ratios (70/30, 75/25, and 21/79 for entry 7 in Table 2 and entries 2 and 4 in Table 3, respectively). Thus, we have here further demonstrated the utility of using acetate anions to catalyze regioselective acetylation of diols and polyols. We believe that many synthetic approaches for obtaining value-added carbohydrate intermediates could be simplified and expanded through the application of this method. As can be seen (Scheme 2), the methyl β-D-taloside **40**, β-D-idoside **41**, β-D-mannoside **42** and β-D-altroside **43** can be efficiently synthesized from compounds **15** and **17** via a double-parallel inversion[55] and a triggered cascade inversion.[45] These two inversion methods were built on the development of nitrite-mediated inversion.[56−58] In addition to removing toxicity concerns, it is evident that the regioselective acetylation method discussed here has several decisive advantages in comparison with the organotin method, for instance in the synthesis of compounds **15** and **17**.

In conclusion, we propose that a dual H-bonding effect plays an important role in the acetylation of diols and polyols, in

dx.doi.org/10.1021/jo501343x | J. Org. Chem. 2014, 79, 8134−8142

Scheme 2. Comparison of Acetate H-Bonding Method and the Organotin Method for the Synthesis of Value-Added Carbohydrate Intermediates[a]

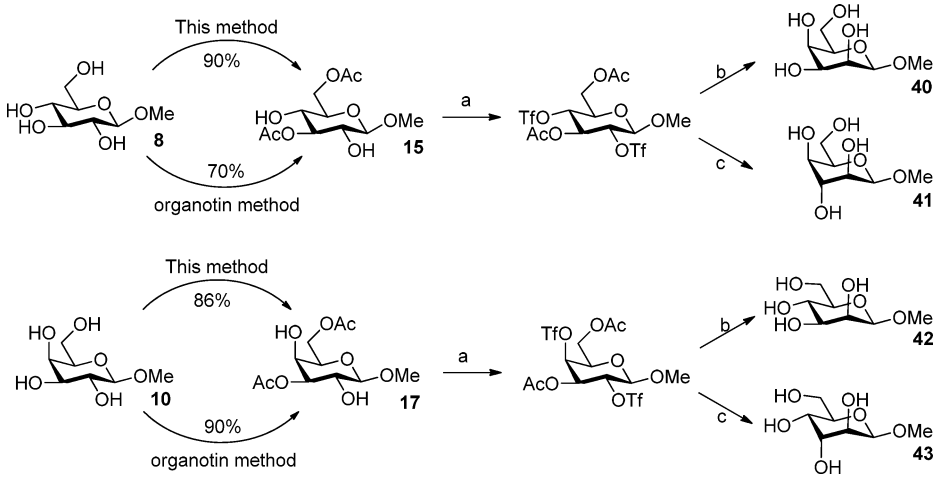

[a]Reaction conditions: reactant (100 mg); (a) Tf_2O, pyridine, CH_2Cl_2, −20 to 10 °C, 2 h; (b) (i) $TBANO_2$, toluene, 50 °C, 5−12 h, (ii) MeONa, MeOH, room temperature, 4 h; (c) (i) $TBANO_2$, EDA, toluene, room temperature, 4 h, then workup with acid, (ii) MeONa, MeOH, room temperature, 4 h.

which hydroxyl groups are first bound to anions through the formation of H bonds. This effect explains why more basic anions provide faster reaction rates in pyridine-catalyzed acetylations. A highly regioselective acetylation of diols/polyols has been developed, in which acetylation is enabled by catalytic amounts of acetate. The overall mechanism and role of acetate has been studied by ^{1}H NMR experiments, quantum chemical calculations, and kinetic isotope effect measurements. Our computational studies suggest that the regioselectivity can be explained by subtle differences in the structure of the competing transition states, where the geometries, or "sterics", are such that reactions at equatorial and primary hydroxyls allow formation of a hydrogen bond, which helps facilitate the regeneration of the acetate catalyst. The regioselectivity is thus controlled by the inherent structure of the diol/polyol−acetate H-bonded complex. To the best of our knowledge, this approach to acetylation offers the most environmentally friendly, convenient, efficient, and regioselective method to date.

EXPERIMENTAL SECTION

General Methods. All commercially available starting materials and solvents were of reagent grade and were dried prior to use. Chemical reactions were monitored with thin-layer chromatography using precoated silica gel 60 (0.25 mm thickness) plates. High-resolution mass spectra (HRMS) were obtained by electrospray ionization (ESI) and Q-TOF detection. Flash column chromatography was performed on silica gel 60 (0.040−0.063 mm). ^{1}H and ^{13}C spectra were recorded with 400 and 100 MHz instruments at 298 K in $CDCl_3$, using the residual signals from *d*-chloroform (^{1}H, δ 7.25 ppm; ^{13}C, δ 77.2 ppm), as internal standard. Assignments were made by first-order analysis of the spectra, supported by standard ^{1}H−^{1}H correlation spectroscopy (COSY). See the Supporting Information for details on the KIE measurements.

General Method for Regioselective Acylation of Polyols. Polyol reactants (100 mg) were allowed to react with acetic anhydride (1.1−2.2 equiv) in dry acetonitrile (1 mL) at 40 °C for 8−12 h in the presence of tetrabutylammonium acetate (0.3−0.6 equiv). The reaction mixture was directly purified by flash column chromatography (hexanes/EtOAc 2/1 to 1/1), affording the pure selectively protected derivatives.

General Method for Obtaining ^{1}H NMR Ratio of Products. Polyol reactants (100 mg) were allowed to react with acetic anhydride (1.1−2.2 equiv) in dry acetonitrile (1 mL) at 40 °C for 8−12 h in the presence of tetrabutylammonium acetate (0.3−0.6 equiv). The reaction mixtures (0.2 mL) were taken and then dried under vacuum. The dried mixtures were directly tested by ^{1}H NMR.

Methyl 3,6-*O*-Acetyl-β-D-glucopyranoside (15).[30] Methyl β-D-glucopyranoside (100 mg) was allowed to react with acetic anhydride (103 μL, 2.1 equiv) in dry acetonitrile (1 mL) at 40 °C for 12 h in the presence of tetrabutylammonium acetate (93 mg, 0.6 equiv). The reaction mixture was directly purified by flash column chromatography (hexane/EtOAc 1/5), affording 119 mg of compound **36** (83%). ^{1}H NMR ($CDCl_3$, 400 MHz): δ 4.95 (m, 1H, H_3), 4.51 (dd, 1H, J_1 = 2 Hz, J_2 = 10 Hz, H_{6a}), 4.36 (dd, 1 H, J_1 = 1.2 Hz, J_2 = 12.4 Hz, H_{6b}), 4.29 (d, 1H, J = 7.6 Hz, H_1), 3.60 (s, 3H, OMe), 3.58−3.41 (m, 3H, H_2, H_4, H_5), 3.15 (s, 1H, 2-OH), 2.60 (s, 1H, 4-OH), 2.36 (s, 3H, OAc), 2.30 (s, 3H, OAc) ppm.

Methyl 3,6-*O*-Acetyl-α-D-glucopyranoside (16).[59] Methyl α-D-glucopyranoside (100 mg) was allowed to react with acetic anhydride (103 μL, 2.1 equiv) in dry acetonitrile (1 mL) at 40 °C for 12 h in the presence of tetrabutylammonium acetate (93 mg, 0.6 equiv). The reaction mixture was directly purified by flash column chromatography (hexane/EtOAc 1.5), affording 112 mg of compound **38** (78%). H NMR ($CDCl_3$, 400 MHz): δ 5.09 (t, 1 H, J_1 = 9.6 Hz, J_2 = 9.6 Hz, H_3), 4.82(d, 1H, J = 4 Hz, H_1), 4.52−4.48 (dd, 1H, J_1 = 4.8 Hz, J_2 = 12.4 Hz, H_{6a}), 4.32−4.29 (dd, 1H, J_1 = 2.4 Hz, J_2 = 8 Hz, H_{6b}), 3.83−3.78 (m, 1H, H_5), 3.66−3.60 (m, 1H, H_2), 3.54−3.47 (m, 4H, H_4, OMe), 3.01 (d, 1H, J = 5.2 Hz, 2-OH), 2.28 (d, 1H, J = 11.2 Hz, 4-OH), 2.18 (s, 3H, OAc), 2.17 (s, 3H, OAc) ppm.

Methyl 3,6-*O*-Acetyl-β-D-galactopyranoside (17).[30] Methyl β-D-galactopyranoside (100 mg) was allowed to react with acetic anhydride (103 μL, 2.1 equiv) in dry acetonitrile (1 mL) at 40 °C for 12 h in the presence of tetrabutylammonium acetate (93 mg, 0.6 equiv). The reaction mixture was directly purified by flash column chromatography (hexane/EtOAc 1/5), affording 120 mg of compound **40** (84%). ^{1}H NMR ($CDCl_3$, 400 MHz): δ 4.86 (dd, 1H, J_1 = 3.2 Hz, J_2 = 10.4 Hz, H_3), 4.36−4.24 (m, 3H, H_1, H_{6a}, H_{6b}), 4.03 (m, 1H, H_4), 3.86−3.81 (m, 1H, H_2), 3.74 (t, 1H, J_1 = 6 Hz, J_2 = 6.8 Hz, H5), 3.57 (s, 3H, OMe), 2.42 (d, 1H, J = 3.2 Hz, 2-OH), 2.34 (d, 1H, J = 5.6 Hz, 4-OH), 2.18 (s, 3H, OAc), 2.09 (s, 3H, OAc) ppm.

Methyl 3,6-*O*-Acetyl-α-D-galactopyranoside (18).[59] Methyl α-D-galactopyranoside (100 mg) was allowed to react with acetic anhydride (103 μL, 2.1 equiv) in dry acetonitrile (1 mL) at 40 °C for 12 h in the presence of tetrabutylammonium acetate (93 mg, 0.6

dx.doi.org/10.1021/jo501343x | J. Org. Chem. 2014, 79, 8134−8142

equiv). The reaction mixture was directly purified by flash column chromatography (hexane/EtOAc 1/5), affording 129 mg of compound **42** (85%). ^{1}H NMR ($CDCl_3$, 400 MHz): δ 5.06 (dd, 1H, J_1 = 3.2 Hz, J_2 = 10.4 Hz, H_3), 4.85 (d, 1H, J = 4 Hz, H_1), 4.35−4.20 (m, 2H, H_{6a}, H_{6b}), 4.02−3.97 (m, 3H, H_2, H_4, H_5), 3.46 (s, 3H, OMe), 2.16 (s, 3H, OAc), 2.08 (s, 3H, OAc) ppm.

Methyl 3-*O*-Acetyl-β-D-xylopyranoside (19).[60] Methyl β-D-xylopyranoside (100 mg) was allowed to react with acetic anhydride (64 μL, 1.1 equiv) in dry acetonitrile (1 mL) at 40 °C for 12 h in the presence of tetrabutylammonium acetate (55 mg, 0.3 equiv). The reaction mixture was directly purified by flash column chromatography (hexane/EtOAc 1/1), affording 117 mg of compound **44** (93%). ^{1}H NMR ($CDCl_3$, 400 MHz): δ 4.81 (t, 1H, J_1 = 12 Hz, J_2 = 12 Hz, H_3), 4.25 (d, 1H, J = 4 Hz, H_1), 4.04 (dd, 1H, J_1 = 4 Hz, J_2 = 4 Hz, H_{5a}), 3.80−3.75 (m, 1H, H_4), 3.54−3.45 (m, 4H, H_2, OMe), 3.36−3.30 (dd, 1H, J_1 = 12 Hz, J_2 = 12 Hz, H_{5b}), 2.17 (s, 3H, OAc) ppm.

1-Acetyl-*O*-propanetriol (20).[20] Propanetriol (50 mg) was allowed to react with acetic anhydride (57 μL, 1.1 equiv) in dry acetonitrile (1 mL) at 40 °C for 8 h in the presence of tetrabutylammonium acetate (98 mg, 0.6 equiv). The reaction mixture was directly purified by flash column chromatography (hexane/EtOAc 1/1), affording 52 mg of compound **45** (71%). ^{1}H NMR ($CDCl_3$, 400 MHz): δ 4.22−4.12 (m, 2H), 3.97−3.92 (m, 1H), 3.73−3.58 (m, 2H), 2.11 (s, 3H) ppm.

Methyl 3-*O*-Acetyl-6-*O*-(*tert*-butyldimethylsilyl)-β-D-glucopyranoside (31). Methyl 6-*O*-(*tert*-butyldimethylsilyl)-β-D-glucopyranoside (100 mg) was allowed to react with acetic anhydride (34 μL, 1.1 equiv) in dry acetonitrile (1 mL) at 40 °C for 12 h in the presence of tetrabutylammonium acetate (30 mg, 0.3 equiv). The reaction mixture was directly purified by flash column chromatography (hexane/EtOAc 1/5), affording 91 mg of compound **31** (81%). ^{1}H NMR ($CDCl_3$, 400 MHz): δ 4.95 (t, 1H, J = 9.5 Hz, H_3), 4.25 (d, 1H, J = 7.8 Hz, H_1), 3.93 (dd, 1H, J_1 = 4.9 Hz, J_2 = 10.5 Hz, H_{6a}), 3.84 (dd, 1H, J_1 = 5.8 Hz, J_2 = 10.5 Hz, H_{6b}), 3.66 (t, 1H, J = 9.5 Hz, H_2), 3.53 (s, 3H, OMe), 3.47−3.35 (m, 2H, H_4, H_5), 2.16 (s, 3H, OAc), 0.89 (s, 9H, *tert*-butyl), 0.08 (s, 6H, $Si(Me)_2$) ppm; ^{13}C NMR ($CDCl_3$, 100 MHz): δ 172.4, 103.8, 77.8, 74.5, 72.3, 71.8, 64.7, 57.4, 26.0, 21.3, 18.4, −5.3 ppm. HRMS (ESI-TOF) m/z: $[M + Na]^+$ calcd for $C_{15}H_{30}O_7SiNa$ 373.1658; found 373.1628.

Methyl 3-*O*-Acetyl-6-*O*-(*tert*-butyldimethylsilyl)-α-D-glucopyranoside (33). Methyl 6-*O*-(*tert*-butyldimethylsilyl)-α-D-glucopyranoside (100 mg) was allowed to react with acetic anhydride (34 μL, 1.1 equiv) in dry acetonitrile (1 mL) at 40 °C for 12 h in the presence of tetrabutylammonium acetate (30 mg, 0.3 equiv). The reaction mixture was directly purified by flash column chromatography (hexane/EtOAc 1/5), affording 86 mg of compound **33** (76%). ^{1}H NMR ($CDCl_3$, 400 MHz): δ 5.06 (t, 1H, J = 9.3 Hz, H_3), 4.72 (d, 1H, J = 3.8 Hz, H_1), 3.88−3.78 (m, 2H, H_{6a}, H_{6b}), 3.66−3.48 (m, 3H, H_2, H_4, H_5), 3.41 (s, 3H, OMe), 2.12 (s, 3H, OAc), 0.87 (s, 9H, *tert*-butyl), 0.06 (s, 6H, $Si(Me)_2$) ppm. ^{13}C NMR ($CDCl_3$, 100 MHz): δ 172.7, 99.4, 76.6, 71.2, 71.0, 70.4, 63.9, 55.4, 26.0, 21.3, 18.4, −5.3 ppm. HRMS (ESI-TOF) m/z: $[M + Na]^+$ calcd for $C_{15}H_{30}O_7SiNa$ 373.1658; found 373.1642.

Methyl 3-*O*-Acetyl-6-*O*-(*tert*-butyldimethylsilyl)-β-D-galactopyranoside (35). Methyl 6-*O*-(*tert*-butyldimethylsilyl)-β-D-galactopyranoside (100 mg) was allowed to react with acetic anhydride (34 μL, 1.1 equiv) in dry acetonitrile (1 mL) at 40 °C for 12 h in the presence of tetrabutylammonium acetate (30 mg, 0.3 equiv). The reaction mixture was directly purified by flash column chromatography (hexane/EtOAc 1/5), affording 91 mg of compound **35** (80%). ^{1}H NMR ($CDCl_3$, 400 MHz): δ 4.81 (dd, 1H, J_1 = 3.1 Hz, J_2 = 10.1 Hz, H_3), 4.23 (d, 1H, J = 7.7 Hz, H_1), 4.16 (d, 1H, J = 3.1 Hz, H_4), 3.96−3.83 (m, 3H, H_2, H_{6a}, H_{6b}), 3.55 (s, 3H, OMe), 3.50 (t, 1H, J = 5.5 Hz, H_5), 2.16 (s, 3H, OAc), 0.87 (s, 9H, *tert*-butyl), 0.07 (d, 6H, $Si(Me)_2$) ppm. ^{13}C NMR ($CDCl_3$, 100 MHz): δ 171.0, 104.4, 75.5, 73.8, 69.5, 68.3, 63.3, 57.2, 26.0, 21.3, 18.4, −5.3 ppm. HRMS (ESI-TOF) m/z: $[M + Na]^+$ calcd for $C_{15}H_{30}O_7SiNa$ 373.1658, found 373.1634.

Methyl 3-*O*-Benzyl-6-*O*-acetyl-β-D-galactopyranoside (36). Methyl 3-*O*-benzyl-β-D-galactopyranoside (100 mg) was allowed to react with acetic anhydride (37 μL, 1.1 equiv) in dry acetonitrile (1 mL) at 40 °C for 12 h in the presence of tetrabutylammonium acetate (32 mg, 0.3 equiv). The reaction mixture was directly purified by flash column chromatography (hexane/EtOAc 1/1), affording 105 mg of compound **36** (91%). ^{1}H NMR ($CDCl_3$, 400 MHz): δ 7.35−7.26 (m, 5 H, Ph), 4.75 (s, 2 H, $PhCH_2$), 4.35−4.33 (m, 2H, H_{6a}, H_{6b}), 4.16 (d, 1H, J = 12 Hz, H_1), 3.94 (s, 1H, H_4), 3.77 (t, J_1 = 8 Hz, J_2 = 8.6 Hz, H_2), 3.63−3.61 (m, 1H, H_5), 3.55 (s, 1H, OMe), 3.46−3.42 (dd, J_1 = 3.2 Hz, J_2 = 9.2 Hz, H_3) 2.08 (s, 1H, OAc) ppm. ^{13}C NMR ($CDCl_3$, 100 MHz): δ 170.8, 137.6, 128.6, 128.2, 127.9, 103.8, 72.1, 80.2, 72.3, 72.2, 70.9, 66.3, 63.0, 56.9, 20.8 ppm. HRMS (ESI-TOF) m/z: $[M + Na]^+$ calcd for $C_{16}H_{22}O_7Na$ 349.1263; found 349.1262.

Methyl 3-*O*-Acetyl-6-*O*-(*tert*-butyldimethylsilyl)-α-D-galactopyranoside (37). Methyl 6-*O*-(*tert*-butyldimethylsilyl)-α-D-galactopyranoside (100 mg) was allowed to react with acetic anhydride (34 μL, 1.1 equiv) in dry acetonitrile (1 mL) at 40 °C for 12 h in the presence of tetrabutylammonium acetate (30 mg, 0.3 equiv). The reaction mixture was directly purified by flash column chromatography (hexane/EtOAc 1/5), affording 89 mg of compound **37** (78%). ^{1}H NMR ($CDCl_3$, 400 MHz): δ 5.02 (dd, 1H, J_1 = 3.1 Hz, J_2 = 10.3 Hz, H_3), 4.82 (d, 1H, J = 3.9 Hz, H_1), 4.17 (d, 1H, J = 2.7 Hz, H_4), 4.05 (b, 1H, H_2), 3.93−3.83 (m, H_{6a}, H_{6b}), 3.74 (t, 1H, J = 4.5 Hz, H_5), 3.41 (s, 3H, OMe), 2.15 (s, 3H, OAc), 0.87 (s, 9H, *tert*-butyl), 0.07 (d, 6H, $Si(Me)_2$) ppm. ^{13}C NMR ($CDCl_3$, 100 MHz): δ 171.3, 100.0, 73.6, 69.5, 69.2, 67.4, 64.0, 55.6, 26.0, 21.3, 18.4, −5.3 ppm. HRMS (ESI-TOF) m/z: $[M + Na]^+$ calcd for $C_{15}H_{30}O_7SiNa$ 373.1658; found 373.1631.

Methyl 3-*O*-Acetyl-6-*O*-(*tert*-butyldimethylsilyl)-α-D-mannopyranoside (38). Methyl 6-*O*-(*tert*-butyldimethylsilyl)-α-D-mannopyranoside (100 mg) was allowed to react with acetic anhydride (34 μL, 1.1 equiv) in dry acetonitrile (1 mL) at 40 °C for 12 h in the presence of tetrabutylammonium acetate (30 mg, 0.3 equiv). The reaction mixture was directly purified by flash column chromatography (hexane/EtOAc 1/5), affording 93 mg of compound **38** (82%). ^{1}H NMR ($CDCl_3$, 400 MHz): δ 5.05 (dd, 1H, J_1 = 3.3 Hz, J_2 = 9.8 Hz, H_3), 4.66 (d, 1H, J = 1.7 Hz, H_1), 4.0−3.81 (m, 4H, H_2, H_4, H_{6a}, H_{6b}), 3.66−3.59 (m, 1H, H_5), 3.36 (s, 3H, OMe), 2.14 (s, 3H, OAc), 0.88 (s, 9H, *tert*-butyl), 0.08 (s, 6H, $Si(Me)_2$) ppm. ^{13}C NMR ($CDCl_3$, 100 MHz): δ 171.4, 100.8, 74.6, 71.6, 69.2, 67.9, 64.5, 55.1, 26.0, 21.3, 18.4, −5.3 ppm. HRMS (ESI-TOF) m/z: $[M + Na]^+$ calcd for $C_{15}H_{30}O_7SiNa$ 373.1658; found 373.1630.

Methyl 3-*O*-Benzyl-6-*O*-acetyl-α-D-mannopyranoside (39). Methyl 3-*O*-benzyl-β-D-mannopyranoside (100 mg) was allowed to react with acetic anhydride (37 μL, 1.1 equiv) in dry acetonitrile (1 mL) at 40 °C for 12 h in the presence of tetrabutylammonium acetate (32 mg, 0.3 equiv) The reaction mixture was directly purified by flash column chromatography (hexane/EtOAc 1/1), affording 100 mg of compound **39** (87%). ^{1}H NMR ($CDCl_3$, 400 MHz): δ 7.35−7.26 (m, 5 H, Ph), 4.78 (d, 1 H, J = 1.6 Hz, H_1), 4.73−4.63 (m, 2H, $PhCH_2$), 4.47−4.43 (dd, 1H, J_1 = 4.8 Hz, J_2 = 12.4 Hz, H_{6a}), 4.32−4.29 (dd, 1H, J_1 = 2.4 Hz, J_2 = 12 Hz, H_{6b}), 4.01 (s, 1H, H_4), 3.81−3.66 (m, 3H, H_2, H_5, H_3), 3.28 (s, 1H, OMe), 2.11 (s, 1H, OAc) ppm. ^{13}C NMR ($CDCl_3$, 100 MHz): δ 171.6, 137.7, 128.7, 128.2, 127.9, 100.6, 72.1, 70.0, 67.8, 66.4, 63.5, 55.0, 20.9 ppm. HRMS (ESI-TOF) m/z: $[M + Na]^+$ calcd for $C_{16}H_{22}O_7Na$ 349.1263; found 349.1263.

■ ASSOCIATED CONTENT

Supporting Information

Text, tables, and figures giving ^{1}H NMR spectra of compounds **15**−**20**, **21a**,**b**, **31**, **33**, and **35**−**38**, ^{13}C NMR spectra of compounds **31**, **33**, and **35**−**39**, the measurement of KIE by ^{1}H NMR experiments, full author list of ref 46, calculated Cartesian coordinates and energies. This material is available free of charge via the Internet at http://pubs.acs.org.

■ AUTHOR INFORMATION

Corresponding Authors

*E-mail for M.R.: martinr@kth.se.

*E-mail for H.D.: hdong@mail.hust.edu.cn.

Notes

The authors declare no competing financial interest.

■ ACKNOWLEDGMENTS

This study was supported by the National Nature Science Foundation of China (Nos. 21272083), the Chutian Project-Sponsored by Hubei Province, and the Project-Sponsored by the SRF for ROCS, SEM. The authors are also grateful to the staff of the Analytical and Test Center of HUST for support with the NMR instruments.

■ REFERENCES

(1) Wang, C. C.; Lee, J. C.; Luo, S. Y.; Kulkarni, S. S.; Huang, Y. W.; Lee, C. C.; Chang, K. L.; Hung, S. C. *Nature* **2007**, *446*, 896−899.
(2) Witschi, M. A.; Gervay-Hague, J. *Org. Lett.* **2010**, *12*, 4312−4315.
(3) Bourdreux, Y.; Lemetais, A.; Urban, D.; Beau, J. M. *Chem. Commun.* **2011**, *47*, 2146−2148.
(4) Chea, E. K.; Fernandez-Tejada, A.; Damani, P.; Adams, M. M.; Gardner, J. R.; Livingston, P. O.; Ragupathi, G.; Gin, D. Y. *J. Am. Chem. Soc.* **2012**, *134*, 13448−13457.
(5) Ferry, A.; Guinchard, X.; Retailleau, P.; Crich, d. *J. Am. Chem. Soc.* **2012**, *134*, 12289−12301.
(6) Grindley, T. B. *Adv. Carbohydr. Chem. Biochem.* **1998**, *53*, 17−142.
(7) Dong, H.; Zhou, Y. X.; Pan, X. L.; Cui, F. C.; Liu, W.; Liu, J. Y.; Ramström, O. *J. Org. Chem.* **2012**, *77*, 1457−1467.
(8) Zhou, Y. X.; Li, J. Y.; Zhan, Y. J.; Pei, Z. C.; Dong, H. *Tetrahedron* **2013**, *69*, 2693−2700.
(9) Xu, H. F.; Lu, Y. C.; Zhou, Y. X.; Ren, B.; Pei, Y. X.; Dong, H.; Pei, Z. C. *Adv. Synth. Catal.* **2014**, *356*, 1735−1740.
(10) Muramatsu, W.; Tanigawa, S.; Takemoto, Y.; Yoshimatsu, H.; Onomura, O. *Chem. Eur. J.* **2012**, *18*, 4850−4853.
(11) Muramatsu, W. *J. Org. Chem.* **2012**, *77*, 8083−8091.
(12) Muramatsu, W.; Takemoto, Y. *J. Org. Chem.* **2013**, *78*, 2336−2345.
(13) Whalen, M. M.; Loganathan, B. G.; Kannan, K. *Environ. Res.* **1999**, *81*, 108−116.
(14) Jenkins, S. M.; Ehman, K.; Barone, S. J. *Dev. Brain Res.* **2004**, *151*, 1−12.
(15) Seinen, W.; Vos, J. G.; van Krieken, R.; Penninks, A.; Brands, R.; Hooykaas, H. *Toxicol. Appl. Pharmacol.* **1977**, *42*, 213−224.
(16) Lee, D.; Taylor, M. S. *J. Am. Chem. Soc.* **2011**, *133*, 3724−3727.
(17) Lee, D.; Williamson, C. L.; Chan, L.; Taylor, M. S. *J. Am. Chem. Soc.* **2012**, *134*, 8260−8267.
(18) Gouliaras, C.; Lee, D.; Chan, L.; Taylor, M. S. *J. Am. Chem. Soc.* **2011**, *133*, 13926−13929.
(19) Zhou, Y. X.; Ramstrom, O.; Dong, H. *Chem. Commun.* **2012**, *48*, 5370−5373.
(20) Pan, X. L.; Zhou, Y. X.; Liu, W.; Liu, J. Y.; Dong, H. *Chem. Res. Chin. Univ.* **2013**, *29*, 551−555.
(21) Gangadharmath, U. B.; Demchenko, A. V. *Synlett* **2004**, 2191−2193.
(22) Wang, H. S.; She, J.; Zhang, L. H.; Ye, X. S. *J. Org. Chem.* **2004**, *69*, 5774−5777.
(23) Dhiman, R. S.; Kluger, R. *Org. Biomol. Chem.* **2010**, *8*, 2006−2008.
(24) Evtushenko, E. V. *Carbohydr. Res.* **2012**, *359*, 111−119.
(25) Griswold, K. S.; Miller, S. J. *Tetrahedron* **2003**, *59*, 8869−8875.
(26) Kawabata, T.; Muramatsu, W.; Nishio, T.; Shibata, T.; Schedel, H. *J. Am. Chem. Soc.* **2007**, *129*, 12890−12895.
(27) Ueda, Y.; Muramatsu, W.; Mishiro, K.; Furuta, T.; Kawabata, T. *J. Org. Chem.* **2009**, *74*, 8802−8805.
(28) González-Sabín, J.; Morán-Ramallal, R.; Rebolledo, F. *Chem. Soc. Rev.* **2011**, *40*, 5321−5335.
(29) Xanthakis, E.; Theodosiou, E.; Magkouta, S.; Stamatis, H.; Loutrari, H.; Roussos, C.; Kolisis, F. *Pure Appl. Chem.* **2010**, *82*, 1−16.
(30) Danieli, B.; Luisetti, M.; Sampognaro, G.; Carrea, G.; Riva, S. J. *Mol. Catal. B: Enzym.* **1997**, *3*, 193−201.
(31) Therisod, M.; Klibanov, A. M. *J. Am. Chem. Soc.* **1987**, *109*, 3977−3981.
(32) Kurahashi, T.; Mizutani, T.; Yoshida, J. *J. Chem. Soc., Perkin Trans. 1* **1999**, 465−473.
(33) Kurahashi, T.; Mizutani, T.; Yoshida, J. *Tetrahedron* **2002**, *58*, 8669−8677.
(34) Kattnig, E.; Albert, M. *Org. Lett.* **2004**, *6*, 945−948.
(35) Spivey, A. C.; Arseniyadis, S. *Angew. Chem., Int. Ed.* **2004**, *43*, 5436−5441.
(36) Nishino, R.; Furuta, T.; Kan, K.; Sato, M.; Yamanaka, M.; Sasamori, T.; Tokitoh, N.; Kawabata, T. *Angew. Chem., Int. Ed.* **2013**, *52*, 6445−6449.
(37) Zhou, Y. X.; Rahm, M.; Wu, B.; Zhang, X. L.; Ren, B.; Dong, H. *J. Org. Chem.* **2013**, *78*, 11618−11622.
(38) Dong, H.; Pei, Z. C.; Byström, S.; Ramström, O. *J. Org. Chem.* **2007**, *72*, 1499−1502.
(39) Williams, J. M.; Richardson, A. C. *Tetrahedron* **1967**, *23*, 1369−1378.
(40) Cheong, P. H.-Y.; Legault, C. Y.; Um, J. M.; Celebi-Olcum, N.; Houk, K. N. *Chem. Rev.* **2011**, *111*, 5042−5137.
(41) Denmark, S. E.; Beutner, G. L. *Angew. Chem., Int. Ed.* **2008**, *47*, 1560−1638.
(42) Xu, S. J.; Held, I.; Kempf, B.; Mayr, H.; Steglich, W.; Zipse, H. *Chem. Eur. J.* **2005**, *11*, 4751−4757.
(43) Steglich, W.; Hofle, G. *Tetrahedron Lett.* **1970**, *54*, 4727−4730.
(44) Hofle, G.; Steglich, W.; Vorbruggen, H. *Angew. Chem., Int. Ed.* **1978**, *90*, 602−615.
(45) Dong, H.; Pei, Z. C.; Ramström, O. *Chem. Commun.* **2008**, *11*, 1359−1361.
(46) Frisch, M. J., et al. *Gaussian 09, Revision A.02*; Gaussian, Inc., Wallingford, CT, 2009 (see the Supporting Information for a full list of authors).
(47) Zhao, Y.; Truhlar, D. G. *Theor. Chem. Acc.* **2008**, *120*, 215−241.
(48) Marenich, A. V.; Cramer, C. J.; Truhlar, D. G. *J. Phys. Chem. B* **2009**, *113*, 6378−6396.
(49) Schwabe, T.; Grimme, S. *Phys. Chem. Chem. Phys.* **2006**, *8*, 4398−4401.
(50) Goerigk, L.; Grimme, S. *Phys. Chem. Chem. Phys.* **2011**, *13*, 6670−6688.
(51) Chai, J.-D.; Head-Gordon, M. *Phys. Chem. Chem. Phys.* **2008**, *10*, 6615−6620.
(52) Mangiatordi, G. F.; Bremond, E.; Adamo, C. *J. Chem. Theory Comput.* **2012**, *8*, 3082−3088.
(53) Zhao, Y.; Truhlar, D. G. *J. Chem. Theory Comput.* **2011**, *7*, 669−676.
(54) Skodje, R. T.; Truhlar, D. G. *J. Phys. Chem.* **1981**, *85*, 624−628.
(55) Dong, H.; Pei, Z. C.; Angelin, M.; Byström, S.; Ramström, O. *J. Org. Chem.* **2007**, *72*, 3694−3701.
(56) Dong, H.; Pei, Z. C.; Ramström, O. *J. Org. Chem.* **2006**, *71*, 3306−3309.
(57) Dong, H.; Rahm, M.; Brinck, T.; Ramström, O. *J. Am. Chem. Soc.* **2008**, *130*, 15270−15271.
(58) Dong, H.; Rahm, M.; Thota, N.; Deng, L.; Brinck, T.; Ramstrom, O. *Org. Biomol. Chem.* **2013**, *11*, 648−653.
(59) Khan, R.; Konowicz, P. A.; Gardossi, L.; Matulova, M.; de Gennaro, S. *Aust. J. Chem.* **1996**, *49*, 293−298.
(60) Evtushenko, E. V. *Synth. Commun.* **2006**, *36*, 1593−1599.